1 High Energy Astrophysics

1.1 Introduction

Theoretical Astrophysics and High-Energy Astrophysics are complementary fields of investigation at the MPI für Kernphysik. Some of the more phenomenological theoretical work is reported here in juxtaposition with the joint projects on Very High Energy γ-ray Astronomy with imaging atmospheric Cherenkov telescopes of the Astrophysics and the Particle Physics divisions of the institute.

In this section of the report, three different areas are addressed:

- The installation of the stereoscopic HEGRA Cherenkov telescope array and its results regarding the detection of cosmic TeV γ-ray sources, the measurement of the cosmic ray proton spectrum, and study of characteristics of electromagnetic air showers;
- The status of the new HESS projects, and its scientific goals;
- The modeling of cosmic γ-ray sources.

1.2 HEGRA System of Atmospheric Cherenkov Telescopes

F. Aharonian, A.G. Akhperjanian[a], M. Aye, K. Bernlöhr, O. Bolz, A. Daum, A. Frass, M. Hemberger, M. Hess, G. Hermann, A. Heusler, I. Jung, R. Kankanyan[a], J. Kettler, C. Köhler, A. Kohnle, A. Konopelko[b], H. Krawczynski, H. Lampeitl, M. Panter, A. Plyasheshnikov[b], G. Pühlhofer, C. Renault, V. Sahakian[a], M. Ulrich, H.J. Völk, C.A. Wiedner, H. Wirth

[a]Yerevan Physics Institute, Armenia

[b]Altai State University, Russia

The buildup of the HEGRA system of five identical IACTs for the investigation of cosmic gamma-rays in the TeV energy range is now complete. The telescopes are operated to observe air showers in coincidence. This stereoscopic viewing allows a 3-dimensional reconstruction of the shower axis, leading to improved directional accuracy, energy resolution, and particle identification. This together with the large field-of-view allows for the first time the observation of extended sources such as young supernova remnants, as well as scans of potentially interesting regions such as the Galactic plane. The observation schedule also included Active Galactic Nuclei, pulsars, and microquasars. In particular, strong flaring of the BL Lac objects Mkn 421 and 501 could be observed. Multi-wavelength (X-ray/TeV) campaigns of these objects have been carried out to understand the acceleration mechanisms in the sources as well as the propagation through the Intergalactic Medium. The Monte Carlo air shower simulation together with a detailed trigger and detector simulation is used to understand characteristics of gamma-ray and hadron air showers, for energy calibration, and for a better particle identification. The Monte Carlo shower characteristics agree to a high precision with the data both for protons and gamma-rays. Furthermore, using a large gamma-ray data sample, it was possible to study air shower properties directly from the data in unprecedented detail.

1.2.1 Installation of the System Telescopes

The HEGRA (High Energy Gamma Ray Astronomy) experiment on the Roque de los Muchachos (2200 m a.s.l.) on the Canary Island of La Palma consists of several detector components dedicated to the study of cosmic rays.

The HEGRA collaboration (MPIK jointly with groups from the MPI für Physik Munich and the Universities of Kiel, Hamburg, Wuppertal, Madrid and Yerevan) built up and currently operates a total of six Cherenkov telescopes on the HEGRA site. Five of the telescopes (CT2 - CT6) are now used as a system, observing air showers in coincidence, the other, the first prototype telescope (CT1), has had major upgrades and is operated as a stand alone instrument.

The HEGRA telescope system consists of the five identical IACTs CT2 through CT6. The telescopes are arranged on the corners of a square with $\sim$100 m by $\sim$100 m area, with one telescope in the center. The MPIK was responsible for the camera mechanics and electronics, the trigger electronics and the data acquisition software. Both the EN-workshop as well as the electronics workshop members of the MPIK were decisive for the development and the buildup of the telescopes on the island.

The first system telescope was built up in summer 1995, the next three telescopes were put into operation during 1996.

In 1997, some hardware changes of the four-telescope system were carried out. The 40 MHz FADC system of CT4 and CT5 was upgraded to the 120 MHz system already installed in the other telescopes. The Kiel group was responsible for the buildup of a local topological next neighbour trigger module, which was added to all telescopes. This made it possible to lower the trigger threshold from 10 mV to 8 mV, corresponding to about 7 photoelectrons. Prior to the installation of the next neighbour trigger the system was run with a two-level trigger, whereby at least two adjacent pixels in each of at least two telescopes need to trigger within a coincidence window of 70 ns [1]. The system trigger rate was 15 Hz, creating about 600 MByte per hour of data.

Other hardware modifications included the installation of new air conditioning in the local electronic huts, due to problems with the air conditioning at high humidity.

In October 1997, a fire damaged part of the HEGRA array as well as the masts and the electronics hut of CT4. Fortunately, the camera and electronics were unharmed. Immediate repair work led to the telescope being operational again only six weeks later. During the repair observations were continued with 3 CTs.

Problems with the initial mirror mounts were solved with modified mirror supports. The tensions exerted on the mirrors are now taken by a reinforced triangle. All broken mirrors were replaced together with modified mirror supports, and none of these replaced mirrors has broken.

The telescope CT2 - the initial prototype of the system telescopes, equipped with a 61-pixel camera - was upgraded with a new camera, electronics, masts and mirrors and incorporated into the data acquisition system of the CT system in August 1998. Thus, the buildup of the CT system is now complete.

In 1997 the mirror dish of the prototype CT1 telescope was equipped with hexagonal Al mirrors increasing the dish area to ~ 10.5 m^2. This work was largely carried out by the Munich group. Since 1997, CT1 has a high resolution 127 pixel camera, built by the Kiel group.

1.2.2 Performance of the telescopes

The system of 4 Cherenkov telescopes (CTs) operated throughout the 13 shift periods in 1997 for the first full year. The shift crew came from all participating HEGRA institutions. From September 1998 onwards, data were taken with 5 CTs in coincidence.

The software of the CT-system was implemented such that observational scans of a celestial region could be performed. Important is that the detailed sequence of observations e.g. after a technical failure or a bad weather are controled by the computer.

CT1 had a separate observation schedule: On short notice targets of interest could be observed. After extended tests by the Munich group this telescope was also used to observe during twilight and moonshine since 1997 - after reducing the voltages of the camera PMTs. The $\sim$20% additional observing time was particularly important for sampling the light curve of the flaring Mkn 501 in both years.

The Hamburg and Wuppertal groups were largely responsible for the implementation of the BACODINE alert system which informs shift operators whenever a strong Gamma Ray Burst is accessible for CT observations.

The efficiency and reliability of the HEGRA CTs has increased during the previous years. Table 1 shows some figures of the operational performance of the CT - system in 1997 and 1998.

1.2.3 Sources of CT observations

The observation program for the CT-system is agreed upon annually in HEGRA collaboration meetings. In 1997 and 1998, 26 potential sources for γ-emission were observed. In addition, in 1998 1 scan and 2 scans in 1997 of extended regions were performed. For CT1, the number of target sources increased from 12 in 1997 to 18 in 1998. Two GRB follow-up observations were done both in 1997 and 1998 with CT1.

Table 2 shows the number of observing hours of the CT - system for the proposed Galactic sources. Due to flaring activity of both BL Lac objects, Mkn 421 and Mkn 501, multiwavelength campaigns were initiated, which included simultaneous observations with satellite detectors - ASM/XTE, BeppoSAX and ASCA - and other terrestrial telescopes. The HEGRA CTs participated in the various campaigns mainly in 1998. In Table 3 observing times for sources are listed which flared also in other wavelength regimes and have been looked at for more than 3 hours.

Proposals were submitted in 1997 to investigate 47 further AGNs, based on their proximity (low z) and X-ray luminosity. In addition, the observation of two galaxies (M 82 and M 87) has been agreed upon. Table 4 shows the observation hours dedicated so far for these targets.

	1997	1998
Total obs. time [h]	1636	1562
CT-system operation [h]	831	1018
Losses		
from bad weather [h]	446	286
from techn. problems [h]	≥ 250	$\sim$110

Tab. 1: *Performance characteristics of the CT - system.*

Source	obs. hrs 1997	obs. hrs 1998
Crab Nebula	92	194
SNR Cas A	102	85
SNR Tycho	23	58
SNR IC 443	25	28
GRS 1915	50	12
SS 433	-	19
Geminga	-	41
Scans of		
Fly's Eye region	18	-
Galactic Plane	111	66

Tab. 2: *Galactic sources observed by the CT - system.*

Source	obs. hrs 1997	obs. hrs 1998
Mkn 421	128	163
Mkn 501	156	150
1ES 2344	19	46
BL Lac	13	7

Tab. 3: *Extragalactic flaring objects observed for more than 3 hours by the CT - system.*

1.2.4 Analysis Techniques

Cherenkov telescopes record the images of extended air showers in the atmosphere, which are induced by primary TeV gamma rays or charged cosmic particles. The showers typically reach their maximum at 8-10 km a.s.l., are several kilometers long, and at the height of La Palma the Cherenkov photons create a light pool on the ground of 250 m diameter.

Stereoscopic images of an air shower, i.e. if the same shower is recorded with several telescopes under different viewing angles, permit an unambiguous reconstruction of the shower di-

Source	obs. hrs 1997	Source	obs. hrs 1998
1ES 0145	4	**1ES 0927**	15
1ES 0229	3	**HB89-2201**	18
1ES 0236	7	**HB89-2254**	9
1ES 0347	4	**NGC 0315**	16
BL 0647	4	**1H 0323**	9
BL 0829	23	**IRAS 13541**	5
BL 1014	6	**0120+340**	15
3C 120	7	**M 82**	21
3C 197.1	4	**NGC 1275**	20
4C 31.04	4		
4C 37.11	7		
1EXO 0706	6		

Tab. 4: *AGNs observed by the CT - system for more than 3 hours.*

rection and the shower impact point. The knowledge of the distances of the shower to the telescopes along with the light images in the cameras allows to reconstruct the shower energy as well as to effectively suppress the large background of cosmic-ray induced showers.

1.2.5 Observation techniques

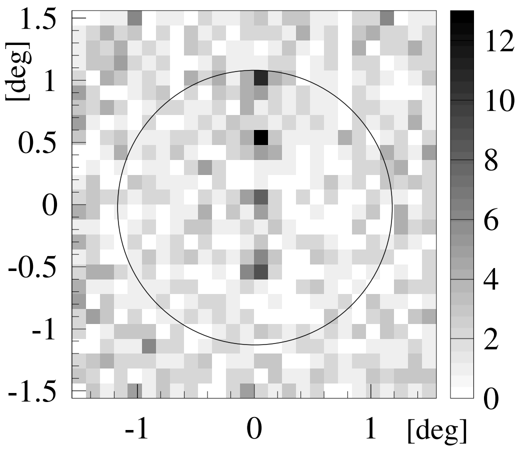

Abb. 1: *Effective field of view of 2° diameter. Shown are the reconstructed particle origins in coordinates of the field of view. Image parameters are used to suppress cosmic ray induced showers. The Crab Nebula was placed at 4 different positions for about 40 min each. In this integrated image the four 'virtual' Crabs can be well detected and separated.*

The effective field of view (FOV) of the telescopes is defined as the area on the sky, where primary gamma rays can come from to be effectively reconstructed. It differs from the optical field of view of the single telescopes, since the latter must contain the extended images (up to $\sim 2^0$)arising from the air showers. The HEGRA System of Cherenkov telescopes has a FOV of $2°$ diameter with homogenous sensitivity for gamma rays (see Fig. 1). This leads to the following advantages:

- Extended sources can be observed for the first time. These are the only sources where the standard ON-OFF observation cycle is still applied. OFF source observations (some degrees next to the source) are needed to get an estimate for the background induced by charged cosmic rays. Typically every 20-30 min ON and OFF positions are switched.
- When observing point sources, given the angular resolution of better than $0.1°$, a large fraction of the FOV can be used to determine the expected background. In order to minimize any systematics caused by slight inhomogeneities inside the FOV, the so-called wobble mode is applied. Here the source is displaced from the center of the FOV, periodically switching between plus and minus $0.5°$ in declination. Run loops are again typically 20-30 min.
- For the first time scans of extended sky regions can be performed with reasonable sensitivity.

1.2.6 Geometric event reconstruction

The camera images are characterized using the standard second moment parametrization [2]. Each image is described by an ellipse of inertia. The shower direction is determined by the intersection of the major axes of two images. If more than two telescopes observe a shower, the direction is the mean of all intersection points weighted with the angle between the intersecting lines, yielding an angular resolution of better than $0.1°$. The shower impact point on the ground is similarly determined in the coordinate system of the telescopes.

1.2.7 Separation of gamma rays from charged cosmic rays

The directional event reconstruction accuracy of $< 0.1°$ determines the point spread function for gamma ray images at the sky (see e.g. Fig 1). When looking for emission from a point source, about 99% of the events in the FOV of the camera can be rejected by the condition that the primary must have come from the direction of the source.

The shape of the light images is then used to further suppress cosmic-ray induced showers. Gamma-ray candidates are selected using the so-called mean scaled width. This is the ratio of the width of the image to the width expected for photon-induced showers, given the distance to the shower, the total number of photoelectrons in the image and the zenith angle. The ratio is averaged over all triggered telescopes. The expected width values are calculated from a Monte Carlo table, using an empirical function to interpolate between zenith angles.

Advanced analysis techniques use more image parameters (e.g. the length of the image) to have a better identification of gamma and charged cosmic rays.

1.2.8 Energy reconstruction

The energy reconstruction uses the fact that, for a given type of primary particle and shower core distance, the density of Cherenkov light at the ground is proportional to the primary particle energy.

Two energy reconstruction algorithms have been developped:

- The first method calculates an energy estimate for each triggered telescope from the size (the total number of photoelectrons in the camera), the shower distance, and the zenith angle [3]. The size distributions assuming photon-induced showers are determined from Monte Carlo simulations.
- The second method uses a maximum likelihood algorithm. The energy is estimated by maximizing the common probability density function $\prod p(size; r, E, \theta)$, with the product over all triggered telescopes. Here θ is the zenith angle, and r is the shower core distance. The probability density functions are again determined from the Monte

Carlo simulations for discrete bins in r, E, and θ.

1.2.9 Reconstruction properties

The quality of the shower reconstruction has been tested directly from the data and compared to Monte Carlo simulations.

The angular resolution for the origin of the primary gamma ray is better than 0.1° per single event [4]. With sufficient statistics, the position of the gamma ray source on the sky can be determined with an accuracy of $\sim 0.01^\circ$ [5].

Dividing the four-telescope system into two groups of two telescopes and looking at the correlation between the shower reconstruction of the two subgroups yields errors in the x-coordinate (and y-coordinate) of the shower core of $\sim$8 m at shower core distances up to 120 m [6].

Using loose image cuts leads to a very homogenous acceptance of gamma rays over a wide range of energies [7], in total 96% of the gammas are accepted while already rejecting 80% of the background. Tightening the image cuts, in order to search for the weakest gamma ray sources, yields a cosmic ray suppression of a factor of 100 while still having a gamma efficiency of up to 40%.

From Monte Carlo simulations, the quality of the energy reconstruction for both of the above methods is $\Delta E/E \sim 20\%$.

Besides the reconstruction methods described above, a χ^2-minimization procedure was investigated [8] [9]. The shower core, shower direction, energy, and height of the maximum are all fit simultaneously by minimizing a χ^2-function that uses the pixel intensities and the lateral and longitudinal light profiles of gamma-ray induced showers as determined by Monte Carlo simulations. The shower direction resolution is improved by 50% and the shower core reconstruction by 45% compared to the conventional reconstruction method.

1.2.10 Characteristics of gamma ray showers

The HEGRA IACT system with its exact determination of the shower geometry, combined with the unprecedented statistics provided by the 1997 Mkn 501 gamma-ray data sample allows to study the characteristics of air showers in unprecedented detail.

As an example, Fig. 2 illustrates the distribution of the intensity of Cherenkov light from TeV gamma-ray showers on the ground [10]. This distribution is the key ingredient in the determination of the effective detection area and hence for the calculation of source spectra.

To measure the distribution of Cherenkov light, the location of the shower core was reconstructed from the stereoscopic observations; for not too distant showers, an accuracy of about 10 m is reached (see section 1.2.4). In the next step, showers of a fixed energy have to be selected, without making explicit assumptions concerning the distribution of Cherenkov light. This is achieved by selecting events with the shower core at a fixed distance from a given "reference" telescope, and requiring a fixed image intensity in this telescope. In a final step, the light yield observed in other telescopes can now be determined as a function of the distance to the shower core. (Note, however, that this technique determines the radial dependence of the Cherenkov light intensity, but not its absolute scale.)

The light distribution was investigated as a function of zenith angle (Fig. 2), and as a function of shower energy (i.e., light intensity in the reference telescope). The data for small zenith angles show a relatively uniform light pool up to distances of 120 m from the core, and a rapid drop for larger distances. The distance of 120 m corresponds to a radius r of photons emitted under the Cherenkov angle θ_c at the height of the shower maximum h_{max}, $r = \theta_c h_{max}$. For larger zenith angles Θ, the diameter of the light pool increases significantly; the reason is that the distance to the shower maximum grows roughly as $1/\cos\Theta$. Also indicated in Fig. 2 are the predictions of detailed Monte-Carlo simulations, including both, the development of the air shower and the properties of the telescopes and cameras. The simulations are in good agreement with the measurements.

With increasing shower energy one observes that the distribution of Cherenkov light develops a peak at small distances to the core. At these higher energies, showers penetrate deeper into the atmosphere, and the Cherenkov light from particles in the tail of the shower is concentrated near the shower core.

The photon density in the radial distribution of Cherenkov light shown above is integrated

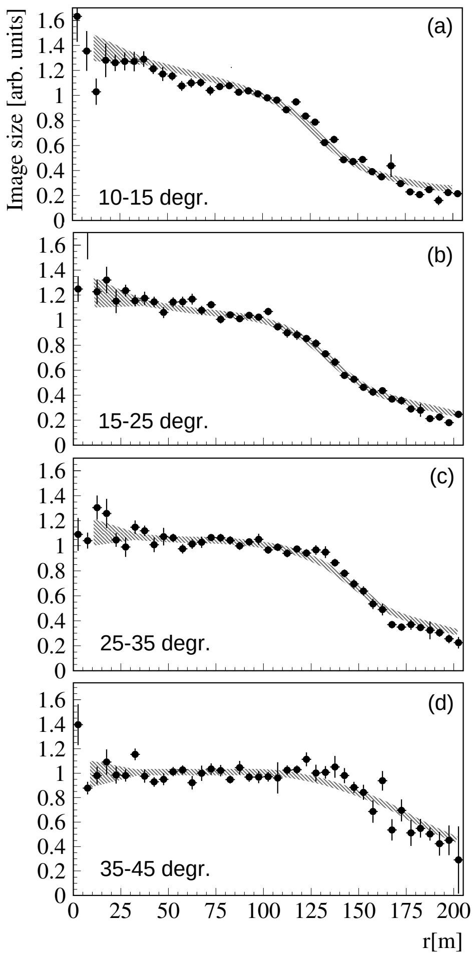

Abb. 2: *Light yield of gamma-ray showers as a function of core distance, for different ranges in zenith angle. The distributions are normalized at a radius of 100 m. Only statistical errors are shown. The shaded bands indicate the results of Monte-Carlo simulations.*

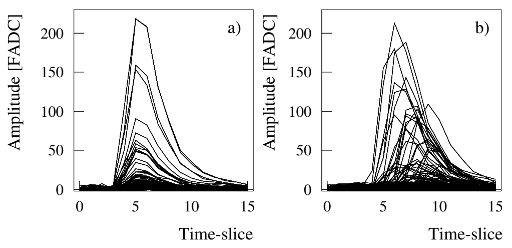

Abb. 3: *Signals recorded by the 120 MHz digitizers of the HEGRA cameras, for two images (a),(b). Signals from all pixels of one camera are superimposed. One time slice corresponds to 8.3 ns.*

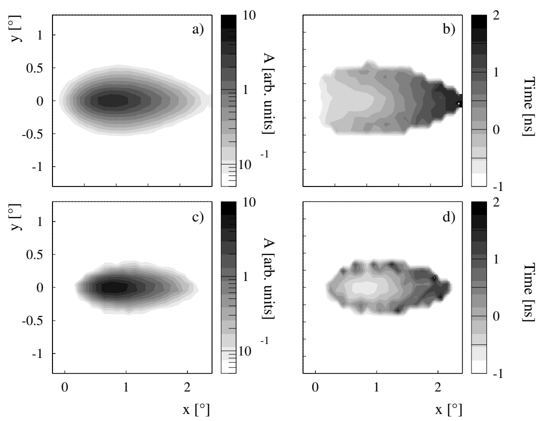

Abb. 4: *Amplitude profiles using logarithmic scales (a),(c) and time profiles (b),(d) of hadronic showers (a),(b) and of gamma-ray showers (c),(d), for core distances d between 100 and 120 m. The profiles were obtained by averaging over many showers, after transforming the images into a common coordinate system, where the x axis denotes the longitudinal axis of the image, roughly equivalent the the height of emission, $x \approx d/h$.*

over all angles of incidence within the field of view of the camera, and over photon arrival times within a certain time window. As a next step, one can now investigate differential distributions in these variables, at fixed distance to the shower core. Work concentrated in particular on the photon arrival time [11], triggered by the observation that, while in most events all camera pixels responded at the same time (Fig. 3a), there was a certain fraction of events with a wide dispersion among photon arrival times (Fig. 3b).

The intensity profiles and timing profiles of images both of cosmic-ray showers and of gamma-ray showers were studied by superimposing, for a fixed core distance and orientation, the images of many showers (Fig. 4).

The amplitude profiles show the expected features: the images are basically elliptical, but not quite symmetric in x with respect to the center of gravity of the images. The gamma-ray images are more compact than the images of cosmic-ray showers. The dominant feature of the timing profiles of hadronic showers is a gradient along x, with a variation of about 3 ns along the image. The effect is less pronounced for gamma-ray images. These effects can be interpreted in a simple geometrical picture [11], and result from an interplay of path lengths of shower particles and of Cherenkov photons, of the speed of propagation of the shower front and of the Cherenkov photons (Fig. 5).

Fig. 6 illustrates how the longitudinal amplitude profiles and time profiles vary with core distance: with increasing distance, images elongate and the gradient of photon arrival times

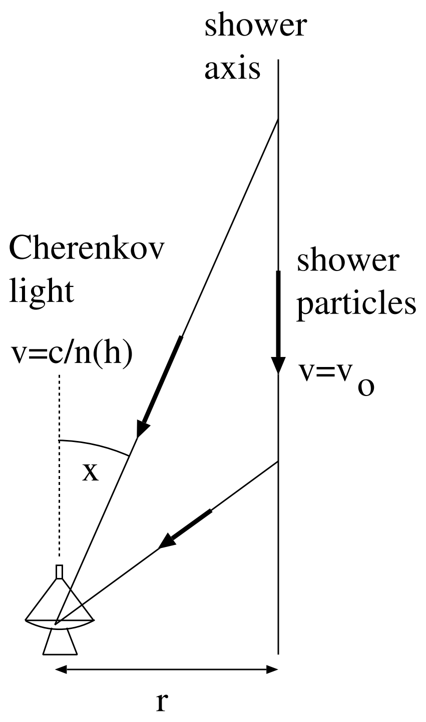

Abb. 5: *Illustration of a simple model used to interpret longitudinal time profiles. Shower particles propagate essentially with the vacuum speed of light in case of gamma-ray showers, and slightly slower in hadronic showers in the TeV energy regime, where nucleon masses cannot be completely neglected. The Cherenkov light propagates with the speed of light in the medium.*

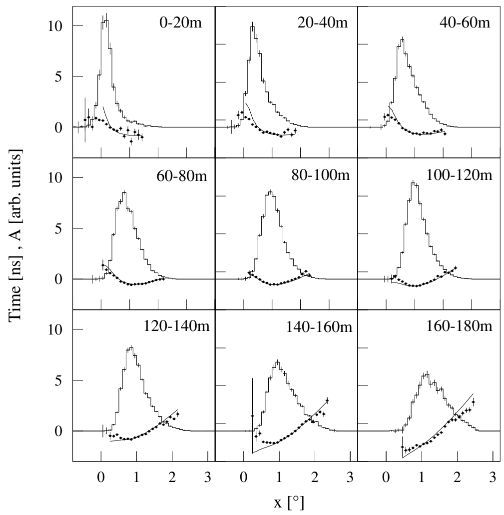

Abb. 6: *Longitudinal profiles, both for image intensities (crosses) and mean photon arrival times (points), for different ranges in core distance. The lines illustrate a simple geometrical model, assuming that the (particle) shower front propagates at the vacuum speed of light.*

increases. Data are reasonably well reproduced by the simple geometrical model.

The observed timing characteristics of shower images have direct relevance for the layout of Cherenkov cameras and their electronics. Given the differences of 5 ns and more in photon arrival times across the images, cameras which use fixed and short integration gates may truncate and deform the images, since photons at both ends of the image arrive outside the gate. On the other hand, one could think of using the differences in timing patterns between cosmic-ray showers and gamma-ray showers as an additional means to reduce the cosmic-ray background. Studies showed, however, that while in principle such a discrimination is possible, the timing characteristics are strongly correlated with the image shape parameters, and little is gained by combining cuts on image shapes, and cuts on timing characteristics. This study influenced the design of the HESS cameras (see section 1.4) using a simple gated integrator which is sufficient for signal recording, rather than a Flash-ADC.

1.2.11 Monte Carlo shower simulations

The Monte Carlo shower simulations are usually used for performance studies of the imaging atmospheric Cherenkov experiments (see e.g. [12]). The measurement of absolute γ-ray flux and energy spectra of the established γ-ray sources as well as the determination of upper limits for the quiet objects heavily rely on Monte Carlo predictions of the detector performance. Here we shortly discuss the results of the detailed Monte Carlo simulations for the complete HEGRA array of 5 imaging air Cherenkov telescopes.

The generation of the air showers has mainly been performed using the ALTAI Monte Carlo code. For the electromagnetic cascade this code has implemented an algorithm based on the analytical probability distributions of the electron (positron) transport. This algorithm substantially reduces the computational time needed for the simulation of a single shower. The proton-nuclei cascade in the atmosphere is simulated according to the radial scaling model based on accelerator data. The air showers induced by the primary nuclei are simulated in a model of independent nucleon interactions for the fragmentation of the projectile-nucleus system. The fragmentation of the colliding nuclei is processed according to the probabilities of different fragmentation channels. We studied the influence of the proton-nuclei cascade model on the observable shower parameters using additional simulations using the CORSIKA code with the HDPM model.

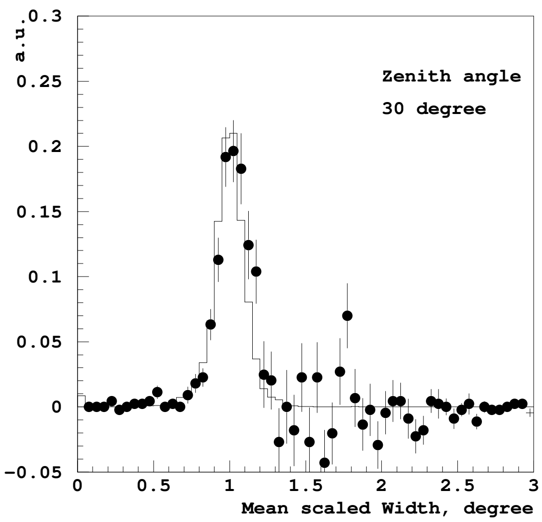

Abb. 7: *Distributions of mean scaled width parameter of the γ-ray-induced air showers detected by the HEGRA IACT array (dots). The histogram shows the results of Monte Carlo simulations.*

The Monte Carlo library contains air showers induced by primary γ-rays, protons, helium and other nuclei belonging to the CNO group, heavy and very heavy nuclei. The primary energy of the showers is distributed within the energy range from 100 GeV to 100 TeV. The simulations have been done for several zenith angles up to 60^0. For each type of primary particle and for each zenith angle approximately 10^5 showers were simulated. Special attention was paid to the proper simulation of the camera and electronics of the HEGRA Cherenkov telescopes [13]. The detector simulation procedure accounts for all efficiencies involved in the process of the Cherenkov light propagation which starts with emission of a Cherenkov photon and ends with the digitization of the PMT signal. The structure of the readout based on the 120 MHz FADC data acquisition and the multiple-telescope trigger scheme were implemented in the simulations. Note, that this procedure takes into account the arrival times of the Cherenkov light photons hitting the telescope reflector.

Detailed comparisons of the detected cosmic ray and γ-ray-induced air showers with simulations were made to understand the performance of the detector [14]. The measured and computed rates are in good agreement which confirms that the trigger procedure has been modelled correctly. The distributions of the shape parameters of the Cherenkov light images from the cosmic ray air showers depend on the model of the development of the proton-nuclei cascade in the atmosphere and also on the model of the nucleus-nucleus interaction. To study this effect the simulations have been performed using the ALTAI and CORSIKA codes (with the HDPM model). The results show good agreement between the two simulation codes, despite of the very different models which are used for the simulations of the proton-nuclei component of the air showers. The long observations ($\simeq$ 110 h) of Mkn 501 in 1997 with the HEGRA system provided for the first time a large data base of γ-rays ($\geq$ 30000 events) with unprecedented signal-to-noise ratio. Several observational key characteristics of γ-ray-induced air showers were measured with small statistical uncertainties. The agreement of these key characteristics of γ-ray induced air showers in experimental data and Monte Carlo simulations substantially strengthened the reliability of the simulations. As an example Fig. 7 shows the measured and simulated distributions of the *mean scaled width* (parameter of the angular lateral size of the image) for γ-ray-induced air showers. The data and simulations are in a very good agreement.

Based on the Monte Carlo simulations we have calculated the basic characteristics of the IACT system [14] which are used in the standard data analysis procedure, i.e. the collection areas, the detection rates, the angular resolution, the energy resolution, and the γ/hadron-separation efficiency etc. Thus the HEGRA system of 5 telescopes with the relatively small mirror area of 5×8.5 m^2 gives a rather low energy threshold of $\simeq$ 500 GeV (see Fig. 8).

The large camera field of view ($\simeq 4.3^0$) allows to perform the observations of point γ-ray sources in the wobble (shifted) source mode taking at the same time ON and OFF events, without lack of sensitivity and increasing the available observation time by a factor of two. The use of several images gives an angular resolution of better than 0.1 degree and a cosmic ray rejection using the shower orientation of up to a factor of 100. The geometrical reconstruc-

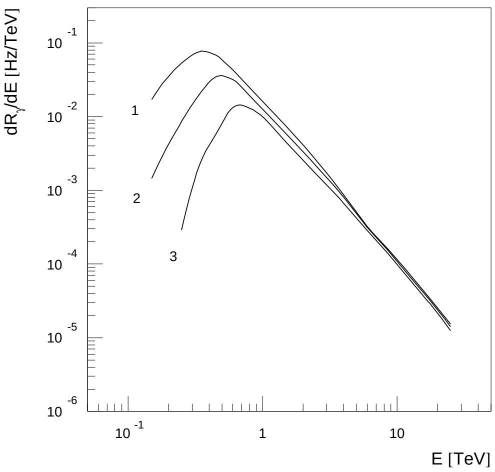

Abb. 8: *The differential detection rates of γ-ray-induced air showers simulated at zenith which are detected by the system of 5 HEGRA IACTs operating with different local trigger thresholds: 2/5,* 2nn/271 > q_0, *with q_0= 8 (1); 10 (2); 14 (3) ph. e. The assumed γ-ray spectrum is a power-law with the spectral index of 2.5 and with a flux normalization chosen as* $J_\gamma(>1\,\mathrm{TeV}) = 10^{-11}\,\mathrm{cm}^{-2}\mathrm{s}^{-1}$.

tion of the shower impact position with good accuracy ($\sim$ 10 m) improves the energy resolution and makes it possible to apply image shape cuts which are independent of the shower energy. The energy reconstruction procedure for the CT-system is straightforward and is not related to the image shape. The energy resolution of the HEGRA system in the dynamic energy range of 0.5 GeV - 30 TeV is better than 20%. In order to avoid the uncertainties in the evaluation of the energy spectrum of the detected γ-rays the effective collection area can be taken simply as the geometrical area around the center of the telescope system using the restriction on the reconstructed impact parameter (e.g. 200 m). Simultaneous registration of several Cherenkov light images from an individual air shower makes it possible to apply the correlated analysis of the image shape (*mean scaled width*) and to substantially improve the cosmic ray rejection. In the "search mode" tight software cuts on shape and orientation show the better performance approaching the case of a background-free detection of γ-ray sources. Note that after application of the strong analysis cuts, the amount of the detected cosmic electrons ($\simeq$ 0.4 particle per hour) becomes comparable to the cosmic ray contamination, so that further suppression of the background is limited by the electron content. For the energy spectrum studies one can use "loose" analysis cuts providing high γ-ray statistics. A 5σ detection of γ-ray fluxes from point sources at the level of $J_\gamma(>1\,\mathrm{TeV}) = 10^{-12}\,\mathrm{cm}^{-2}\mathrm{s}^{-1}$ is possible in 20 hours of observations.

1.2.12 The TeV γ-ray spectrum of the Crab Nebula

The Crab Nebula has been extensively observed and studied over an enormously broad photon energy range embracing the radio, optical, X-ray bands as well as high energy γ-rays up to tens of TeVs. The predicted spectrum in the TeV energy domain appears to be very sensitive to the theoretical scenarios of photon emission: the value of magnetic field, the nature of seed photons, the maximum energy of electrons, etc. Thus a measurement of the TeV Crab spectrum sets major constraints on theoretical expectations.

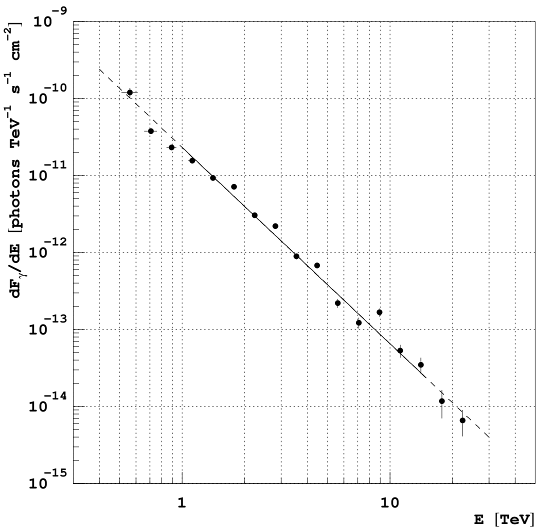

Abb. 9: *The energy spectrum of the Crab Nebula.*

The imaging air Cherenkov technique was used for observations in the TeV energy range. Currently the Crab serves as a standard candle for TeV γ-ray emission. However the Crab energy spectrum, as measured by several groups, still differs in power-law slope as well as in absolute normalization. In addition the energy spectrum measurements are usually affected by systematic errors, limiting the accuracy of the result. Stereo imaging gives several advantages for studies of the spectrum compared to single telescope data: (a) the direct measurement of the shower impact parameter; (b) a good energy resolution; (c) a wide dynamic range; (d) extended capabilities for systematic studies using several images of an individual shower. The Crab Nebula were observed by the HEGRA stereoscopic system of 4 imaging air Cherenkov telescopes (IACTs) for about 100 hours from September 1997 to March 1998 [15]. The recent detailed studies on the system performance give an energy threshold and an energy resolution for γ-rays of 500 GeV and $\sim$ 20%, respectively. The Crab spectrum was measured with the IACTs system in the very broad energy range from 500 GeV to 25 TeV, using the observations at zenith angles up to 50 degree. The effective detection areas, the acceptances after analysis cuts were inferred from Monte Carlo simulations as described in section 1.2.6. The Crab data were analyzed with the recently developped technique of energy spectrum evaluation. The Crab energy spectrum is shown in Fig. 9 [15]. The data can be fitted by a simple power law over the energy range 1-20 TeV, which yields

$$dJ_\gamma(E)/dE = (2.7 \pm 0.2 \pm 0.8) \cdot 10^{-7}$$
$$\left(\frac{E}{1\,\mathrm{TeV}}\right)^{-2.61 \pm 0.06 \pm 0.1} \mathrm{m}^{-2}\mathrm{s}^{-1}\mathrm{TeV}^{-1}.$$

The first set of errors is statistical and the second is estimated using the Monte Carlo simulations which also take into account the current uncertainties in absolute calibration of the detector. The data does not exclude a possible slight steepening of the energy spectrum usually predicted by inverse Compton modeling of the TeV γ-ray emission. A simple power law fit of the Crab data over the energy range taking into account the energy range below 1 TeV yields a differential spectrum index of $\sim$ 2.45, which indicates a flatter spectrum. However, the noted change of the energy spectrum slope is within the current statistical and systematic errors and the data over the quoted energy range are consistent with a simple power law fit. Our data match well at about 20 TeV the recent data published by the CANGAROO group, which extend up to 70 TeV and are consistent with a flat power law index of $\sim$ 2.5 beyond 10 TeV, which is likely for TeV γ-rays due to π^0s, generated by protons accelerated at the termination shock of the pulsar wind.

1.2.13 Measurement of the energy spectrum of the cosmic ray protons

The HEGRA system of 4 IACTs has been used to determine the flux and the spectrum of cosmic ray protons over a limited energy range around 1.5 TeV [16]. Although the IACT system is designed for the detection of γ-rays with energies above 500 GeV, it also has a large detection area of $\sim 10^6\,\mathrm{m}^2 \cdot 3\,\mathrm{msr}$ for primary protons of energies above 1 TeV and the capability to reconstruct the primary proton energy with a reasonable accuracy ΔE/E $\sim$ 0.5 near the threshold. The stereoscopic detection of the air showers permits the effective suppression of air showers induced by heavier primary particles already on the trigger level, and in addition by the software analysis cuts. The combination of both capabilities permits a determination of the proton spectrum almost independently of the cosmic ray chemical composition [17].

In the analysis the data sample of the Mkn 501 observations from 1997 was used. It contains a large fraction of data at small zenith angles ($\leq 20°$) and does not contain any bright star which causes excessive additional noise. The strong γ-ray beam was excluded from the analysis by rejecting all showers reconstructed within 0.3° from the source. We have applied the forward folding method for the proton spectrum evaluation. Detailed Monte Carlo simulations were used in the analysis. The best fit to the data in the energy range from 1.5 to 3 TeV yields [16]

$$dJ_p/dE = (0.11 \pm 0.02_{\mathrm{stat}} \pm 0.05_{\mathrm{sys}})$$
$$(E/1\,\mathrm{TeV})^{(-2.72 \pm 0.02_{\mathrm{stat}} \pm 0.15_{\mathrm{sys}})}\,\mathrm{s}^{-1}\mathrm{sr}^{-1}\mathrm{m}^{-2}\mathrm{TeV}^{-1}$$

The differential energy spectrum is shown in Fig. 10. The systematic error of the spectral index is dominated by the Monte Carlo dependence of the results and by the contamination of the data sample with heavier particles. The systematic error of the absolute flux is affected in addition by an uncertainty in the energy scale of 15 %.

Our results are in very good agreement with the recent results of satellite and balloon-borne experiments. The new technique yields a similar accuracy as achieved with other experiments of the proton spectrum. It gives as best fit a power-law with the integral index of 1.72. Earlier claims about a possible cutoff in the proton spectrum at energies $\simeq 10$ TeV are clearly not confirmed by our measurements. The future development of the analysis technique will provide us with the opportunity to study the energy spectrum and fluxes of the heavier CR nuclei and set an independent constraint on the chemical composition of the cosmic rays.

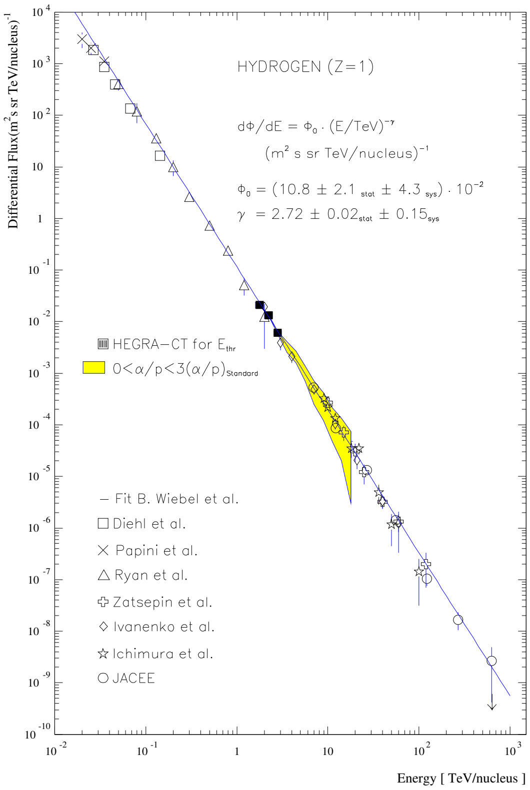

Abb. 10: *Compilation of the proton spectrum measurements. The black points identify the measurements by the HEGRA IACT system. The shaded area represents the systematic error for two limiting values of Helium/proton nuclei ratio in primary CRs,* $\alpha/\mathrm{p} = 0$ *(upper curve) and* $3(\alpha/\mathrm{p})_{\mathrm{standard}}$*, with* $(\alpha/p)_{standard} = 0.61$ *(lower curve).*

1.2.14 Galactic sources

A major part of the observation program of the IACT system was dedicated to the search for TeV emission from Galactic objects. The target catalogue comprised supernova remnants, pulsars and microquasars. Due to the extended field of view (see section 1.2.4), the system is uniquely able to look at extended sources (e.g. some supernova remnants) which are completely contained in the field of view of the camera. Moreover it is also possible to scan parts of the sky with reasonable sensitivity; this was for the first time performed on parts of the Galactic disc shown in Fig. 11.

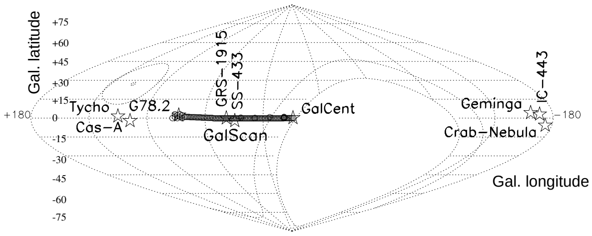

Abb. 11: *The sky in Galactic coordinates; the Milky Way would show up as a horizontal disc of some degrees in width in this picture. Shown are the positions of the objects described below. The oval shaped white area is not visible from La Palma, the band surrounding that region can only be observed under limited conditions.*

1.2.15 Supernova remnants

Immediately after the partial commissioning of the stereoscopic system in the late summer of 1996, the observation of the supernova remnant (SNR) $G78.2 + 2.1$ (also called γ-Cygni) was started. The observation of another SNR, IC 443, was started in December 1996 with the then existing 4-telescope system. In the case of $G78.2 + 2.1$ only data from a 3-telescope configuration were used for the analysis, amounting to 47.5 h ON-time and 25.1 h OFF-time, after data selection according to weather conditions and stability of the system components. For IC 443 the corresponding times are 10.8 h for ON, and 10.8 h for OFF.

Both SNRs are shell remnants from the core collapse of massive stars with a progenitor wind (SN II). They are very well investigated in many other wavelength ranges. For IC 443, with a radius of 0.375°, there are strong indications for an interaction of the SNR with neighbouring dense clouds; for γ-Cygni, with a radius 0.51°, there is no such physical indication despite persuasive “visual” impressions of such an interaction. Obviously both SNRs are extended sources for a Cherenkov telescope.

Despite the relative long observation time for γ-Cygni no γ-ray signal could be detected. The upper limit (which is consistent with a corresponding Whipple upper limit) lies considerably below the extrapolation of the EGRET detection below 1 GeV, and also not insignificantly below the theoretical estimates for the expected nuclear γ-ray emission (cf. Drury et al. 1994, A&A, v.287, p.959; Berezhko and Völk 1997, Astroparticle Physics, v. 7, p. 183). The explanation may lie in the fact that the EGRET radiation stems from the pulsar at that position whose spectrum is expected to turn down after a few tens of GeV. For IC 443 the connecting power law of the EGRET fluxes and the HEGRA CT system upper limit is only marginally too steep to be acceptable for the source spectrum of the Galactic Cosmic Rays. Also the HEGRA 0.8 TeV upper flux limit is only a factor of 0.6 below the theoretically expected nuclear γ-ray flux, and is as well consistent with the Whipple upper limit at 300 GeV. While for γ-Cygni no further detection efforts with the HEGRA system seem warranted, this may not be true for IC 443. (The observations of IC 443 in 1998 are not yet analysed.)

Two pointlike supernova remnants, Cas-A and Tycho SNR, have been extensively looked at in 1997 and 1998 to search for emission at the level of 1% of the Crab flux. Preliminary analyses of the 1997 data encouraged us to continue these observations in 1998. A final data analysis is under way.

1.2.16 Pulsars

Two millisecond pulsars, the Crab and the Geminga pulsar, have been examined for pulsed TeV emission [18]. For this, a GPS receiver was installed in December 1997. Before, the accurate event time (200 ns level) was provided by the atomic clock of the HEGRA scintillator array synchronized with another GPS receiver. Now two independent time measurements are available. Extensive checks have been performed to test the reliability of the hardware event times as well as the software packages which are needed to transform the event times into the rest frames of the pulsars.

The analyses of the two sources represent the basic aims in the search for pulsed emission.

The Crab is an established steady emitter of TeV gammas. If part (or all) of the emission would be found to be pulsed, this would give information about the extension of the emission region and possibly also about particle acceleration processes in the source.

The data sample contains ≈83 hrs of observation time, with ≈3000 accepted gamma rays. Fig. 12 a) shows the ON-source data (dots) as

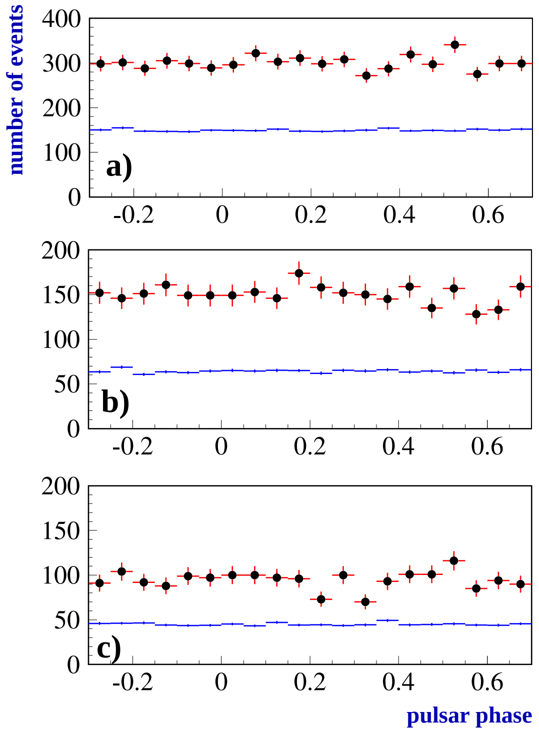

Abb. 12: *Observed number of events from the direction of the Crab depending on the Crab pulsar phase. The dots with error bars are ON-source observations, the dashes are background estimates derived from OFF-source observations with extended angular acceptance. a) total data sample; b) reconstructed primary energy <1TeV; c) reconstructed primary energy >1TeV.*

well as the backgound estimates (dashes), subdivided into time slices in fractions of the known Crab pulsar phase. The background shows no pulsed emission as expected, but also the ON-source observations are consistent with an unpulsed flux. No more than 2.3% (3σ C.L.) of the DC flux is coming as additional pulsed emission, using the 10% time slice in the 30 MeV - 10 GeV band where EGRET detects the most prominent pulsed peak.

Fig. 12 b) and c) show similar analyses, now dividing the data into a high and a low energy subset. In this way, a pulsed population of TeV gamma rays having a different spectrum from the DC spectrum can also be ruled out.

The Geminga pulsar has not been detected in the TeV region so far. Hence an analysis of the events coming from the Geminga position serves to enhance the signal (gammas) to noise (cosmic rays) ratio. Consequently the detection capability of the instrument is enlarged in case of pulsed TeV emission from this object.

The used data set comprises about 13 hrs, the derived upper limits are 13% of the Crab flux assuming a DC flux, and 7.2% of the Crab flux assuming pulsed emission in the phase fraction where EGRET measures pulsed emission in the GeV band.

1.2.17 Microquasars

Microquasars are the galactic miniature analogues of AGNs, the central object being either a black hole or a neutron star. The emission jets often show apparent superluminal motion.

GRS 1915+105 has been a source of special interest for HEGRA since analysis of the CT2 standalone telescope data of 1995 and 1996 showed marginal evidence for TeV emission [4]. It is possible that the source shows episodic emission, which was also slightly favoured by the data. The IACT system was used in 1997 and the beginning of 1998 to continously monitor the source. Preliminary data analysis showed so far no hints for TeV emission during that time period.

Another microquasar, SS 433 (W 50), was observed during 1998. Including the jet stuctures it has an apparent extension of about $2^\circ \times 1^\circ$ at optical wavelengths. This makes the source still suitable for the IACT system, though with some difficulties.

1.2.18 Galactic plane scan

Usually, Cherenkov telescopes are used to observe sources which are well established in other wavelenghbands. The limited sensitivity of present instruments leads to the fact that most of the sky has never been examined in the TeV band.

The HEGRA CT-system is for the first time able to perform scans with a sensitivity for point sources well below the Crab flux. Reasons are the high angular resolution of 0.1°, a homogeneously sensitive field of view of $\sim 4^\circ$ diameter, and a quasi background-free detection of TeV gammas of the instrument.

As the first target for such a scan, a part of the Galactic disk was examined. The observations extended from the Galactic center to the local arm of our Galaxy, where the sun is located. This region was chosen because of the high concentration of supernova remnants and other Galactic objects; but also yet unknown sources would be of high interest. The EGRET catalog in the adjacent GeV waveband also shows a population of sources, of which no counterparts have been identified yet. As the most ambitious task one can search for diffuse TeV emission from the Galactic disk.

The campaign took about 100 hrs of observation time in 1997 and 30 hrs in 1998. The 1997 data has been preanalyzed, and showed no significant hints for strong TeV point sources. Analysis techniques will be improved, especially for the region around the Galactic center, which is difficult to observe at La Palma due to the large zenith angles.

1.3 BL Lac objects Mkn 501 and Mkn 421

The discovery of more than 50 γ-ray emitting AGNs by the Compton Gamma Ray Observatory demonstrates that the high energy γ-radiation above 100 MeV is a common feature of blazars – AGNs with relativistic jets directed almost along the observer's line of sight. In the case of BL Lac objects – a sub-class of relatively nearby blazars characterized by weak emission lines – the energy spectrum extends up to TeV energies. The spectral energy distribution (SED) of two BL Lac objects, Mkn 421 and Mkn 501, spans 18 decades in frequency, from GHz radio to multi-TeV γ-rays. It has a characteristic shape with two pronounced peaks at X-ray and TeV γ-ray energies. The absolute intensity in both X-ray and TeV channels exhibits correlated flares within timescales $\Delta t \leq 1\,\mathrm{day}$. This is interpreted as a strong argument in favor of the synchrotron-Compton models which assume that the X-rays and TeV γ-rays have a common origin, i.e. they are produced in the jet due to the synchrotron radiation and inverse Compton scattering of the *same* population of very high energy electrons. Therefore, it is believed that the TeV γ-radiation combined with X-ray observations is likely to be the most informative window to study the highly non-stationary processes of particle acceleration and their radiation in AGN jets. It is important that the current sensitivity of the HEGRA system of 5 IACTs, $f_{\mathrm{E}} = 10^{-11}\,\mathrm{erg/cm^2 s}$ ($\approx 1/4$ Crab) for 1 hour of observation time, nicely fits [19] the range of flux variations of the two strongest BL Lac objects in TeV γ-rays, Mkn 421 and Mkn 501 - from a typical flux f_{E} =0.1 to 0.2 Crab at the quiescent state to $f_{\mathrm{E}} \sim 10$ Crab during strong flares. Therefore the detailed study of the temporal and spectral characteristics of Mkn 421 and Mkn 501 was one of the highest priority objectives of the HEGRA collaboration in 1997 and 1998. In 1998 this study was conducted within several successful multiwavelength campaigns with satellite-borne X-ray detectors on RXTE, ASCA, and BeppoSAX. The time windows of the satellite observations were chosen essentially from the condition of the visibility of Mkn 421 and Mkn 501 by the HEGRA telescopes. In particular, fully simultaneous X-ray/TeV observations with a total duration of more than 100 ksec were performed during the multiwavelength campaign of Mkn 421 in April 1998 (HEGRA/ASCA/BeppoSAX), and the multiwavelength campaign of Mkn 501 in June (HEGRA/RXTE). The analysis of the data from different instruments and the interpretation of the results of these multiwavelength observations are in progress. Meanwhile, recently we completed the study of the temporal and spectral characteristics of Mkn 501 based on the observations with the HEGRA IACT system during the extraordinary activity of this source in 1997.

Mkn 501 is a faint source of TeV γ-radiation with a typical average flux not exceeding 1/4 of the Crab flux. But in 1997 it turned into a state of activity, unique in both its strength and duration. The multi-TeV emission of the source from March to September 1997 was characterized by a strongly variable flux exceeding on average by a factor of three the flux of the Crab Nebula, the strongest known persistent TeV source on the sky.

The observations of Mkn 501 during this remarkable outburst by the HEGRA stereoscopic IACT system resulted in a detailed study of the temporal and spectral characteristics of the source based on unprecedented (more than 30,000) TeV photon statistics [20, 21, 7, 22, 23].

The "background-free" detection of γ-rays with an average rate of several hundred γ-rays per 1 hour (against ≈ 20 background events caused by cosmic rays) allowed us to reveal statistically significant signals every ≤ 5 minutes during the entire 6 months of observations. More importantly, we were able to monitor the energy spectrum of the source on a daily (or shorter) basis. The differential spectra obtained for 4 exemplary individual nights are shown in Fig. 13 [7]. One of the important conclusions of that study is that despite the strong flux variability of emission on timescales ≤ 1 day, the energy spectrum appeared to be rather stable, showing a power-law shape at energies between 1 and several TeV, but with gradual steepening at higher energies [21, 7, 22, 23]. In order to study the correlation between the flux intensity and the differential spectrum we show in Fig. 14 the spectra averaged over 3 groups of data: (1) the whole data set, (2) data corresponding to low (≤ 3.5 Crab) and (3) high (≥ 7 Crab) fluxes, respectively. Within the statistical errors the shapes of all three spectra are very similar.

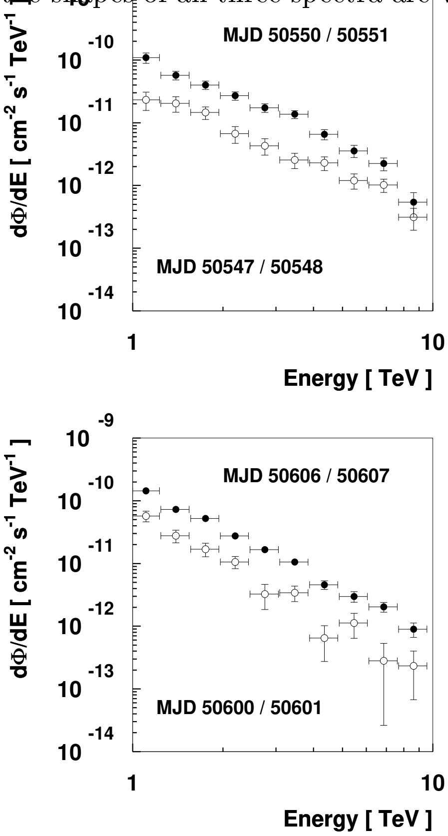

Abb. 13: *The γ-ray spectra of Mkn 501 for 4 individual nights. For each of the 2 observation periods in March/April, and May/June, 1997, a night of weak emission and a night of a strong emission has been chosen. MJD 50550 corresponds to 12 April, 1997.*

This is not a trivial conclusion. Generally, in these highly dynamical objects, when the flux could be changed by more than an order of magnitude within 1 day of observations, strong time variation of the emission spectrum seems to be natural. In the framework of inverse Compton origin of TeV radiation, the lack of correlation between the spectral shape and absolute flux could be explained as result of (1) a time-independent spectrum of acceleration of electrons, and (2) a very fast radiative (synchrotron and inverse Compton) cooling of electrons which establishes an equilibrium spectrum of electrons during the time required for the collection of sufficient photon statistics. The requirement of fast radiative cooling of TeV electrons is in agreement with the typical parameters characterizing the jets in BL Lac objects and also explains the observed dramatic flux variability of X-rays and TeV γ-rays on timescales less than several hours.

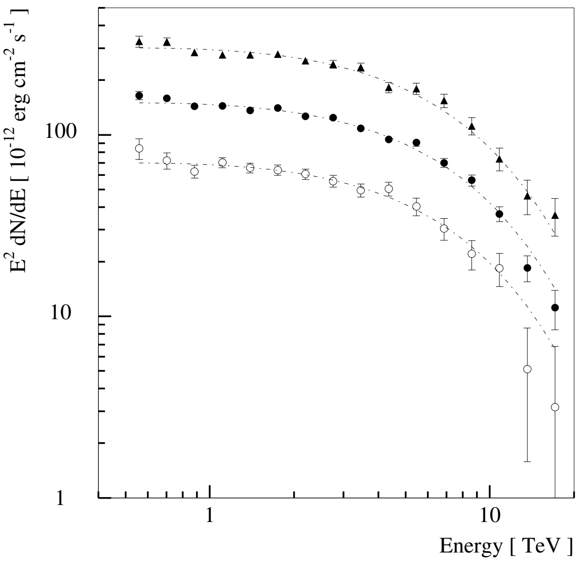

Abb. 14: *The time average SED ($E^2 \cdot dN/dE$) of Mkn 501 in 1997, averaged over 3 different data sets: all nights of observations (dots), only nights with a flux less than 3.5 Crab (open circles), and only nights with a flux more than 7 Crab (triangles).*

Actually the absence of time variability of the shape of the γ-ray spectrum could also be naturally explained by hadronic models of γ-radiation, assuming that γ-rays have a "π^0" origin, i.e. they are produced by interactions of accelerated protons with the ambient gas. Yet the efficiency of this mechanism in the jet appears to be too low to explain the observed time variability and the high fluxes of TeV radiation.

Besides different important constraints on the parameters characterizing the AGN jets, the low correlation between spectral shape and absolute flux has an important practical implication allowing an extension of the spectrum below 1 TeV and beyond 10 TeV. Indeed, the shortage of adequate photon statistics in both energy bands (at low energies - basically due to the drop of the detector's collection area, and at high energies - due to the steep photon spectrum) can be *formally* compensated by using data accumulated over the whole period of observations. Obviously, such superposition of data obtained from a highly variable source can be justified only by the absence of an apparent *flux-spectrum* correlation.

The large photon statistics combined with a 20% energy resolution of the instrument yields a smooth average differential spectrum (see Fig. 15) which can be approximated between 1 TeV and 25 TeV as $dN/dE \propto E^{-1.9}\exp(-E/6.2\,\mathrm{TeV})$. A χ^2-analysis gives a 2σ lower limit on the minimum photon energy of the signal of 18 TeV. We would like to emphasize the uniqueness of the obtained differential spectrum, even by the standards of more advanced branches of modern astronomy, in the sense that it is well determined in the deep exponential regime up to energies $E \sim 3\,E_0$.

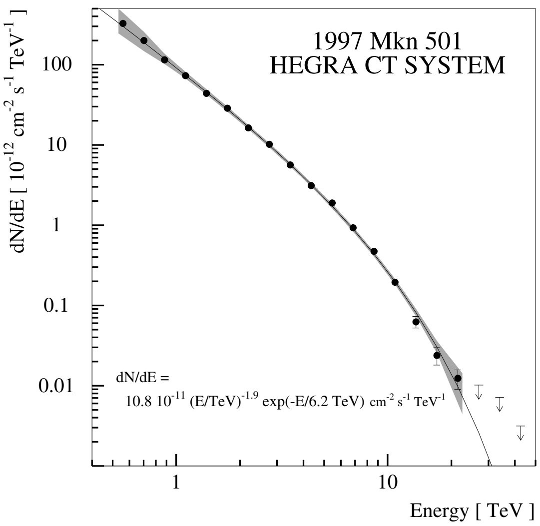

Abb. 15: *The time averaged differential spectrum of Mkn 501 in 1997.*

The detection of TeV γ-rays from Mkn 501 makes the conclusion unavoidable that the observed γ-radiation is produced in the relativistic jet. Otherwise the TeV γ-rays could not escape the source due to severe γ-γ absorption inside the source in interactions with soft radiation fields. The optical depth $\tau_{\gamma\gamma}$ of the source strongly depends on the so-called Doppler factor δ_j of the moving source, $\tau_{\gamma\gamma} \propto \delta_\mathrm{j}^6$. This allows us to constrain the jet Doppler factor to $\delta_\mathrm{j} \geq 10$. Actually, the opposite choice would be to interpret the detected spectrum of Mkn 501 as a power law, but modified by internal γ-γ absorption. This would give an accurate determination of the jet's Doppler factor, $\delta_{\rm j} = 8.5$. However, since there could be other reasons for the steepening of the TeV spectrum, this estimate can only be considered as a robust lower limit on δ. In particular, the steepening of the γ-ray spectrum at the highest energies could be attributed either to an exponential cutoff in the spectrum of accelerated particles, as well as to a deformation of the primary spectrum during the propagation of TeV γ-rays through the diffuse extragalactic background radiation (DEBRA). The very fact that the spectrum of Mkn 501 extends beyond 10 TeV gives a meaningful upper limit on DEBRA in the mid IR wavelength region between 5 and 20 microns, $\epsilon^2 n(\epsilon) \sim 10^{-3}\,\mathrm{eV/cm^3}$. Since this limit is rather close to the current theoretical/phenomenological estimates of DEBRA, it would be very important to derive the absolute fluxes based on the TeV data. However our current poor knowledge about the intrinsic spectrum of Mkn 501 does not allow us to make any definite conclusions about the effect of the intergalactic absorption of TeV γ-rays. And *vice versa*, the uncertainty in the density of DEBRA does not allow us to take into account the intergalactic absorption effect, and thus to "reconstruct" the intrinsic γ-ray spectrum. The knowledge of the latter is an obvious condition for a quantitative study of the acceleration and radiation processes in the source. Therefore we believe that real progress in this field can only be achieved by the analysis of both the spectral and temporal characteristics of X-ray and TeV γ-ray emissions obtained during multiwavelength campaigns that investigate several X-ray selected BL Lac objects at different states of activity, and located at different distances within several 100 Mpc. We hope that the successful multiwavelength campaigns of Mkn 421 and Mkn 501 in 1998 with participation of several X-ray satellites and the HEGRA IACT system will provide the first interesting results in this area.

[1] N. Bulian, A. Daum, G. Hermann, M. Hess, W. Hofmann, H. Lampeitl, G. Pühlhofer, C. Köhler, M. Panter, M. Stein, G. Boerst, G. Rauterberg, M. Samorski, C. Sauerland, and W. Stamm, "Characteristics of the Multi-Telescope Coincidence Trigger of the HEGRA IACT System", Astroparticle Physics 8, pp. 223-233 (1998).

[2] Annual Report MPIK Heidelberg, p.80, 1994

[3] C.Köhler, "Entwicklung einer Methode zur Bestimmung der Energie kosmischer TeV-Gamma-Quanten mit den Tscherenkow-Teleskopen der HEGRA-Kollaboration - Das Energiespektrum der aktiven Galaxie Mrk 501", PhD Thesis, Heidelberg, 1998

[4] Annual Report MPIK Heidelberg, 1996

[5] Pühlhofer G., Daum A., Hermann G., et al., "Locating TeV γ-ray sources with subarcminute precision: the pointing calibration of the HEGRA system of Imaging Atmospheric Cherenkov Telescopes", 1997, Astroparticle Physics 8, pp. 101-108

[6] W.Hofmann, "Measuring Gamma-Ray Energy Spectra with the HEGRA IACT System" Talk given at Workshop "Towards a Major Atmospheric Cherenkov Detector V", Kruger Park, South Africa, 8.-11. Aug. 1997 p. 284-292

[7] Aharonian F., Akhperjanian A.G., Barrio J.A., et al., "The Temporal Characteristics of the TeV Gamma-Radiation from Mkn501 in 1997, I: Data from the Stereoscopic Imaging Atmospheric Cherenkov Telescope System of HEGRA, 1998, accepted by A&A, preprint astro-ph/9808296

[8] M.Ulrich, "Eine neue Bildanalysemethode für Abbildende Atmosphärische Cherenkov Teleskope und die zweidimensionale Richtungsrekonstruktion von TeV Photonen des Krebs-Nebels", PhD thesis, Heidelberg, 1996

[9] I.Jung, "Methoden zur Bildverarbeitung und Ereignisrekonstruktion des HEGRA- Teleskopsystems", Diploma Thesis, Heidelberg, 1999

[10] F. Aharonian, A.Akhperjanian, J. Bario et al. "Measurements of the radial distribution of Cherenkov light generated by TeV γ-ray air showers" , 1999, Astroparticle Physics 10, pp. 21-29.

[11] M. Hess, K. Bernlöhr, A. Daum et al. "The time structure of Cherenkov images generated by TeV γ-rays and by cosmic rays", 1999, Astroparticle Physics, in press.

[12] A.Konopelko "Space-angular and temporal parameters of Cherenkov light emission in air showers of energy from 1 TeV down to 10 GeV", Talk given at Workshop "Towards a Major Atmospheric Cherenkov Detector V", Kruger Park, South Africa, 8.-11. Aug. 1997 p. 208-222.

[13] M. Hemberger "Untersuchung der primären geladenen kosmischen Strahlung oberhalb 1 TeV mit den Methoden der abbildenden Čerenkov-Technik", PhD thesis, Heidelberg, 1998.

[14] A. Konopelko, M. Hemberger, F.Aharonian et al. "Performance of the Stereoscopic System of

the HEGRA imaging Air Čerenkov Telescopes: Monte Carlo Simulations and Observations", Astroparticle Physics, 1999, in press.
[15] A. Konopelko (HEGRA collaboration) "The energy spectrum of TeV gamma rays from the Crab Nebula", Proc. 16th ECRS, Universidad de Alcala, 523, 1998.
[16] F. Aharonian, A.Akhperjanian, J. Bario et al. "The cosmic ray proton spectrum determined with the imaging atmospheriv Cherenkov Technique", Phys. Rev D, 1999, in press.
[17] A. Plyasheshnikov, A. Konopelko, F. Aharonian et al. "Study of mass composition and energy spectrum of primary cosmic radiation by the imaging atmospheric Cherenkov technique", J. Phys. G, Nucl. Part. Phys. , v. 24, p. 653-672, 1998.
[18] F. Aharonian et al., Phase-resolved TeV Gamma-Ray Characteristics of the Crab and Geminga pulsars, submitted to A&A
[19] F. Aharonian (HEGRA collaboration) "On the potential of the HEGRA IACT array", Proc.of 4th Compton Symposium, AIP Conf. Proc., New York, v.2, p.1631-1635, 1997.
[20] F. Aharonian, A.Akhperjanian, J. Bario et al. "Measurement of the flux, spectrum, and time variability of TeV gamma rays from Mkn 501 during a state of high activity", A & A, v. 327, p.L5-L8, 1997.
[21] F. Aharonian, A.Akhperjanian, J. Bario et al. "Study of the Temporal and Spectral Characteristics of TeV gamma radiation from Mkn 501 during a state of high activity by the HEGRA IACT array", Proc.of 4th Compton Symposium, AIP Conf. Proc., New York, v.2, p.1397-1401, 1997.
[22] H. Krawczynski (HEGRA collaboration) "Study of the TeV emission from Mkn 501 with the Stereoscopic Cherenkov Telescope System of HEGRA", Proc. of Turku Conference on the BL Lac Phenomenon, 1999, in press.
[23] A. Konopelko (HEGRA collaboration) "The TeV spectrum of Mkn 501 as measured during the high state in 1997 by the HEGRA stereoscopic system of imaging air Čerenkov telescopes", Astroparticle Physics, 1999, in press.